In Situ Live Cell Sensing of Multiple Nucleotides Exploiting DNA/RNA Aptamers and Graphene Oxide Nanosheets

ARTICLE *in* ANALYTICAL CHEMISTRY · JUNE 2013

Impact Factor: 5.64 · DOI: 10.1021/ac400858g · Source: PubMed

7 AUTHORS, INCLUDING:

Zhaohui Li
Zhengzhou University
23 PUBLICATIONS **1,354** CITATIONS
SEE PROFILE

Thomas J Weber
Pacific Northwest National Laboratory
51 PUBLICATIONS **733** CITATIONS
SEE PROFILE

Dehong Hu
Pacific Northwest National Laboratory
89 PUBLICATIONS **4,676** CITATIONS
SEE PROFILE

Yuehe Lin
Washington State University
364 PUBLICATIONS **21,422** CITATIONS
SEE PROFILE

analytical chemistry

Article

pubs.acs.org/ac

In Situ Live Cell Sensing of Multiple Nucleotides Exploiting DNA/RNA Aptamers and Graphene Oxide Nanosheets

Ying Wang,[†,‡,⊥] Zhaohui Li,[‡,§,⊥] Thomas J. Weber,[‡] Dehong Hu,[‡] Chiann-Tso Lin,[‡] Jinghong Li,*[,†] and Yuehe Lin*[,‡]

[†]Department of Chemistry, Beijing Key Laboratory for Microanalytical Methods and Instrumentation, Tsinghua University, Beijing, China 100084

[‡]Pacific Northwest National Laboratory, Richland, Washington 99352, United States

[§]College of Chemistry and Molecular Engineering, Zhengzhou University, Zhengzhou, China 450001

Supporting Information

ABSTRACT: Nucleotides, for example, adenosine-5′-triphosphate (ATP) and guanosine-5′-triphosphate (GTP), are primary energy resources for numerous reactions in organisms including microtubule assembly, insulin secretion, ion channel regulation, and so on. In order to advance our understanding of the production and consumption of nucleoside triphosphates, a versatile sensing platform for simultaneous visualization of ATP, GTP, adenosine derivates, and guanosine derivates in living cells has been built up in the present work based on graphene oxide nanosheets (GO-nS) and DNA/RNA aptamers. Taking advantage of the robust fluorescence quenching ability, unique adsorption for single-strand DNA/RNA probes, and efficient intracellular transport capacity of GO-nS, selective and sensitive visualization of multiple nucleoside triphosphates in living cells is successfully realized with the designed aptamer/GO-nS sensing platform. Moreover, GO-nS displays good biocompatibility to living cells and high protecting ability for DNA/RNA probes from enzymatic cleavage. These results demonstrate that the aptamers/GO-nS-based sensing platform is capable of selective, simultaneous, and in situ detection of multiple nucleotides, which hold a great potential for analyzing other biomolecules in living cells.

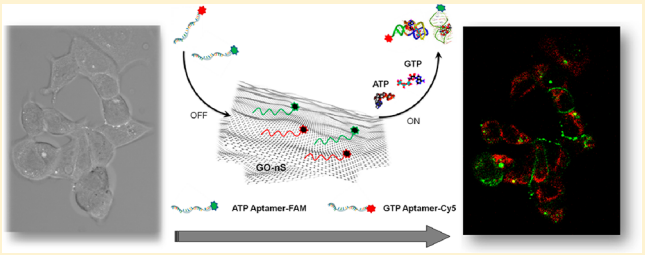

Nucleotides, consisting of a nucleobase and a five-carbon sugar as well as one phosphate group, are mainly considered as the basic building block units in nucleic acids. However, some nucleotides also have many other important roles in metabolism and in metabolic control. Among them, adenosine-5′-triphosphate (ATP) and guanosine-5′-triphosphate (GTP) are found as typical energy molecules regulating various biological processes.[1,2] As the primary energy molecule in living cells, ATP is generally called as the "molecular unit of currency" for intracellular energy transfer,[3−5] which is highly necessary for some biochemical reactions such as muscle contraction, biomolecule synthesis and degradation, membrane transportation, and signal transduction, etc.[6−9] Meanwhile, GTP plays important roles in protein synthesis and holds great significance for signal transduction in living cells.[10−13] Most importantly, ATP and GTP could act coordinately to realize numerous reactions such as microtubule assembly, insulin secretion, and ion channel regulation.[14−17] Therefore, the analysis, especially in situ simultaneous visualization of ATP and GTP, has great importance to advance our understanding of their behavior, function, and interaction inside living cells.[18−21]

In the past decades, numerous attempts have been made to realize the detection of either ATP or GTP. For example, biosensors based on fluorescent molecules like acridine, polythiophene, or imidazolium anthracene derivate have been used for ATP detection.[22−24] Luciferase (an ATP-consuming enzyme) and lymphoid ecto-adenylate kinase have been combined to measure cellular ATP levels in some cases. In addition, ATP aptamer sensors making use of fluorescent, electrochemical, and colorimetric methods have been reported in previous studies.[25,26] Similarly, synthesized fluorescent dyes, such as water-soluble imidazolium anthracene derivative and benzimidazolium with unique specificity, have been applied for GTP detection in buffer solutions as well as biological fluids.[19,21,27] However, most of the assays could only detect ATP or GTP, respectively. Lack of methods is an obstacle to realize the simultaneous detection of ATP and GTP inside living cells. Accordingly, a suitable in situ analyzing assay for multiple biotargets in living cells is highly desirable.

In recent years, graphene oxide (GO) has been emerging with several unique properties including planar sheet structure, fluorescence quenching ability, easy functionalization, and good biocompatibility.[28−32] For example, GO has been utilized for the ultrasensitive detection of cyclin A_2 with a detection limit of

Received: March 22, 2013
Accepted: June 11, 2013
Published: June 11, 2013

   dx.doi.org/10.1021/ac400858g | *Anal. Chem.* 2013, 85, 6775−6782

0.5 nM, 10-fold better than that using single-walled carbon nanotubes.[33] Meanwhile, poly(ethylene glycol) (PEG) modification is also under investigation to extend GO as an anticancer therapeutic drug delivery agent.[34] On the basis of the robust fluorescence quenching ability, GO has been used in fluorescence resonance energy transfer (FRET) applications when combined with either single-strand DNA probes or thrombin aptamers labeled with fluorescence molecules.[35−37] Besides, He et al. has reported a GO-based multicolor fluorescent DNA nanoprobe that allows rapid, sensitive, and selective detection of multiple DNA targets in buffer solutions.[38] Moreover, our previous efforts to develop a proof-of-concept analyzing assay for small-molecule detection in living cells has been reported.[30] This assay has employed modified GO-nS (graphene oxide nanosheets) as a fluorescence quencher and cellular carrier for ATP detection in living cells. The demonstrated dramatic delivery, protection, and sensing abilities should facilitate the development of this technology to be a robust candidate for many other small-molecule detections inside living cells.

Herein, we further applied GO-based sensing technology for simultaneous cellular imaging of adenosine derivates and guanosine derivates to address the issues mentioned above. To validate the utility of this technology in our study, we employed fluorescent dye labeled DNA/RNA aptamers and GO-nS to create an ATP, GTP, adenosine derivates, and guanosine derivates sensing platform. Taking the advantages of aptamers and GO-nS, ATP- and GTP-selective aptamer probes could be loaded onto GO-nS and delivered through cell membrane successfully. Due to the electron acceptor effect of GO-nS, obvious fluorescent off/on switch and real-time target detection in living cells was realized by the aptamer/GO-nS sensing platform. In addition, GO-nS shows excellent protection for DNA/RNA from enzymatic cleavage and good biocompatibility to living cells in the studies. The primary achievements indicated that this GO-nS based sensing system owned promising abilities for monitoring and imaging of multiple nucleotides in living cells, which will enable it to be applied to cellular simultaneous imaging studies of many other predicting biomarkers such as mRNAs and microRNAs.

EXPERIMENTAL SECTION

Materials. Fluorophore carboxyfluorescein (FAM)-labeled ATP aptamer (5′-FAM/AAC CTG GGG GAG TAT TGC GGA GGA AGGT-3′), cyanine-5 (Cy5)-labeled GTP aptamer (5′-Cy5/GGG ACG AAG UGG UUG GGU GUG AAA ACG UCC C-3′), and AF546-labeled random DNA (5′-AF546/TCT AAA TCG CTA TGG TCG C-3′) were synthesized by Integrated DNA Technologies, Inc. (San Diego, CA). Agarose, 10 base-pair DNA ladder, 10× Tris/borate/EDTA (TBE) buffer, gel loading buffer (TrackIt cyan/yellow loading buffer), SYBR green nucleic acid gel stain, DNase I along with the reaction and stop buffers, and trypan blue 0.4% were from Invitrogen (Carlsbad, CA). Adenosine 5′-triphosphate (ATP) disodium salt hydrate, guanosine 5′-triphosphate (GTP) disodium salt hydrate, cytidine 5′-triphosphate (CTP) disodium salt, thymidine 5′-triphosphate (TTP) sodium salt, and all other chemicals including graphite, $K_2S_2O_8$, P_2O_5, and H_2SO_4 were purchased from Sigma-Aldrich (St. Louis, MO). All buffers and reagent solutions were prepared with water purified on a Barnstead NANOPure UV ultrapure water system (Boston, MA). Binding buffer for ATP and GTP assay was 10 mM potassium phosphate with 200 mM KCl, 5 mM $MgCl_2$, and 0.1 mM EDTA.

Preparation and Characterization of GO-nS. Chemically synthesized GO powder was produced by filtrated the production and dried then in vacuum overnight at 25 °C. A 0.2 mg/mL GO aqueous solution was prepared with presynthesized GO powder and sonicated in a water bath for 2 h followed by a strong sonication with power of 40 W (4 min/sonication × 5 sonications) in an ice bath. The ice bath was changed after each treatment to maintain sample temperature below 5 °C. The crude GO was redissolved in 5 M NaOH and sonicated in a water bath for 2 h, followed by adding HCl, and completely rinsed with pure water to natural pH. The obtained GO sample was then autoclaved at 80 °C for 60 min. The autoclaved solution was centrifuged at 12 000 rpm for 10 min, and the supernatant was designated as GO-nS.

Characterization. Atomic force microscopy (AFM) imaging was prepared by first treating a freshly cleaved mica surface with 1 M $MgCl_2$ for 1 min, followed by addition of 10 μL of a sample solution onto the mica surface. The mica substrate was tilted to allow the droplet to spread on the surface. After adsorption for 1 min, the mica surface was washed twice with doubly distilled water and dried with compressed air. The sample was then scanned in tapping mode with a Nanoscope III, Digital Instrument AFM. Transmission electron microscopy (TEM) images of GO-nS and ATP aptamer−FAM/GO-nS were taken on a JEOL TEM 2010 microscope. Powder X-ray diffraction (XRD) measurements were performed on Bruker D8-Advance X-ray powder diffractometer using a graphite monochromator with Cu Kα radiation (k = 1.5406 Å). Raman spectra were obtained using a confocal microprobe Raman system Renishaw, RM200 (Gloucestershire, United Kingdom) using green (514 nm) laser excitation. The Fourier transform infrared spectroscopy (FT-IR) spectrum (800−4000 cm^{-1}) was measured using a Perkin-Elmer Fourier transform infrared spectroscopy spectrometer with pure KBr as the background.

Nucleotides Detection with Aptamer/GO-nS Complex. Solutions of 100 nM ATP aptamer−FAM and/or GTP aptamer−Cy5 were incubated with different concentrations of GO-nS aqueous solution in 10 mM potassium phosphate with 200 mM KCl, 5 mM $MgCl_2$, and 0.1 mM EDTA for 5 min at 25 °C to form the aptamer/GO-nS complex.[39,40] Herein, the 10 mM potassium phosphate with 200 mM KCl, 5 mM $MgCl_2$, and 0.1 mM EDTA was reaction buffer for in vitro detection of nucleotides. The aptamer/GO-nS was tested to determine the quenching ability of GO-nS. The in vitro detection of GTP based on GTP aptamer−Cy5/GO-nS was carried out by adding different concentrations of GTP into 100 nM GTP aptamer−Cy5/GO-nS in reaction buffer, incubating for 1 h at 25 °C, and the mixture solution was scanned on a fluorometer.[41,42] Selective responding of different triphosphates was carried out by incubation of 100 nM ATP aptamer−FAM/GTP aptamer−Cy5/GO-nS complex with 0.5 and 2 mM ATP, GTP, CTP, and TTP in reaction buffer for 1 h at 25 °C by recording the respective fluorescence intensity of the FAM channel and Cy5 channel. In addition, 0.5 and 2 mM ATP and GTP mixture solution was added into the 100 nM ATP aptamer−FAM/GTP aptamer−Cy5/GO-nS complex for the selectivity tests. All of the in vitro detections were recorded on a Tecan Safire 2 microplate reader (TECAN, Switzerland) directly without any other treatments and operations.

Electrophoresis Investigation. Agarose was prepared with 10 mM TBE buffer containing 2 mM EDTA (TBE, pH

dx.doi.org/10.1021/ac400858g | Anal. Chem. 2013, 85, 6775−6782

Scheme 1. Schematic Illustration of the Multiple Sensing Platform[a]

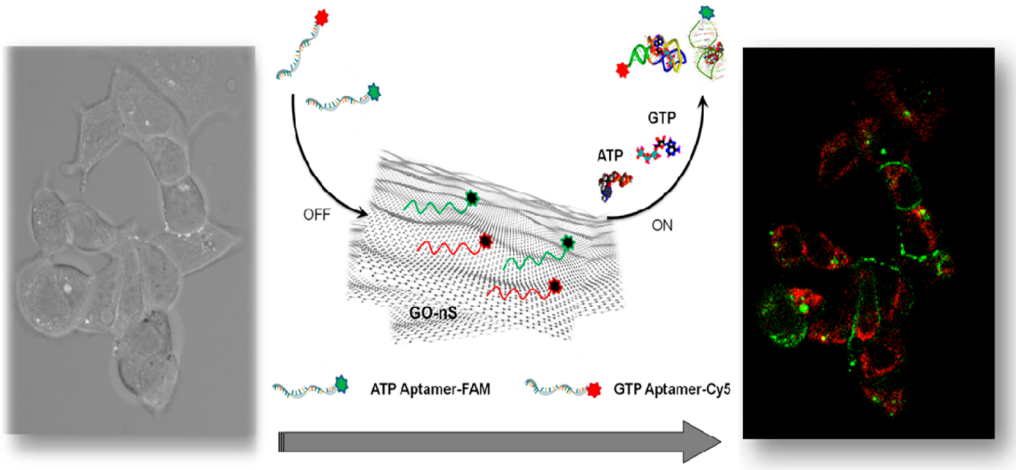

[a]Binding of ATP aptamer−FAM and GTP aptamer−Cy5 to GO-nS led to fluorescence off due to the FRET effect between fluorophores and GO-nS. After incorporating the analytes (ATP or GTP), loop-structured assemblies of aptamer−ATP and aptamer−GTP were released from GO-nS and resulted in fluorescence on. In situ simultaneous probing of ATP and GTP in living cells was realized consequently by using this fluorescence off/on switch concept.

9.2) and heated to form 3.5% agarose−TBE sol−gel. The prepared gel was cooled down to room temperature prior to electrophoresis. An amount of 100 nM of FAM-ATP aptamer, free in solution and unbound to GO-nS, was prepared in DNase I reaction buffer and incubated with 0.2 units/μL of DNase I for 15 and 40 min at room temperature, respectively. The digestion reaction for ATP aptamer−FAM/GO-nS complex was carried out by adding 0.2 units/μL of DNase I into 100 nM aptamer solution premixture with 3 μg/mL GO-nS for 5 min and then incubating for 15 and 40 min, respectively. All samples were heated at 95 °C for 5 min immediately followed by addition of loading buffer prior to gel electrophoresis. Gel electrophoresis was performed in 10 mM TBE buffer at 100 V for 1 h. After electrophoresis, the gel was stained by 5000-fold diluted SYBR green nucleic acid gel stain in 10 mM TBE for 30 min. Then the gel was visualized via NucleoVision imaging system using UV irradiation. Images were captured using GelExpert 2.0 software.

Cell Viability Assay of MCF-7 Cell Incubated with GO-nS. A human breast cancer cell line MCF-7 (ATCC, HTB-22) was grown in the complete Eagle's Minimum Essential Medium (completed EME medium, ATCC) with 0.01 mg/mL bovine insulin and 10% fetal bovine serum (FBS). Cells were grown to confluence in an incubator with humidified atmosphere of 5% CO_2 and 95% air at 37 °C and kept in a confluent state for 24 to 48 h before subculture. The cell culture methods were used for all of the cell studies in the present work. MCF-7 cells were trypsinized and seeded at 5×10^4 cells/well into 12-well flat-bottomed plate. After seeding for 24 h, MCF-7 cells were treated with 1−9 μg/mL GO-nS for 12, 24, and 72 h, respectively. Cell viability was determined using a standard trypan blue cell viability assay (0.05% trypan blue staining for 5 min).

In Situ Live Cell Imaging of Multiple Nucleotides. For in situ investigations, MCF-7 cells were incubated with ATP aptamer−FAM, GTP aptamer−Cy5, and random DNA−Alex546N in the presence or absence of GO-nS at 37 °C for 6 h in 5% CO_2 atmosphere. To form the aptamer/GO-nS complex, aptamers labeled with fluorophore were diluted to 5 μM in reaction buffer. A 1 mg/mL GO-nS aqueous solution was injected into the aptamer buffer to get a final concentration depending on aptamer concentrations. Then the aptamer/GO-nS complex solution was diluted in 1 mL of culture medium (completed EME medium, ATCC) to get the final concentrations of 25, 50, 100, and 200 nM, respectively, for the cell imaging tests. After incubation with aptamer/GO-nS complex, cells were washed with phosphate buffer saline (PBS) completely and images were captured by confocal microscopy on a Zeiss LSM 710 NLO laser scanning confocal microscope with an upright Zeiss Axioexaminer stand. The objective is a W Plan-Apo 20× NA1.0 water dipping objective. The maximum excitation (Ex) wavelength and maximum emission (Em) wavelength for ATP aptamer−FAM are 495 and 520 nm (shown in green color), for GTP aptamer−Cy5 they are 650 and 670 nm (shown in red color), and for random DNA−Alex546N they are 556 and 573 nm (shown in orange color).

RESULTS AND DISCUSSION

Configuration of the DNA/RNA Aptamer/GO-nS Sensing Platform. The basic concept of the proposed sensing platform is shown in Scheme 1. GO-nS and DNA/RNA aptamers were employed to construct the aptamer/GO-nS sensing platform. Aptamers are short, single-stranded oligonucleotides selected by an in vitro method known as SELEX (systematic evolution of ligands by exponential enrichment).[43] As we know, ATP aptamer has been demonstrated with expected performances from fundamental studies to therapeutic researches.[44−46] However, there were no successful reports about GTP aptamer until a novel RNA aptamer with high specificity for the GTP molecule was reported by Szostak and co-workers recently.[47−50] This RNA aptamer is able to target GTP by forming a loop structure with K_d's ranging from 9 nM to 8 μM. On the basis of the previous studies, the multiple sensing platform is constructed through the assembly of DNA/RNA aptamers on GO-nS. Large surface-to-volume ratio and the planar structure of GO-nS provided a suitable substrate for multiple probes assembling. FAM-labeled ATP aptamer and Cy5-modified GTP aptamer were introduced to generate multiple signals corresponding to different targets. The assembly was induced by "$\pi-\pi$ stacking" between aptamers

dx.doi.org/10.1021/ac400858g | Anal. Chem. 2013, 85, 6775−6782

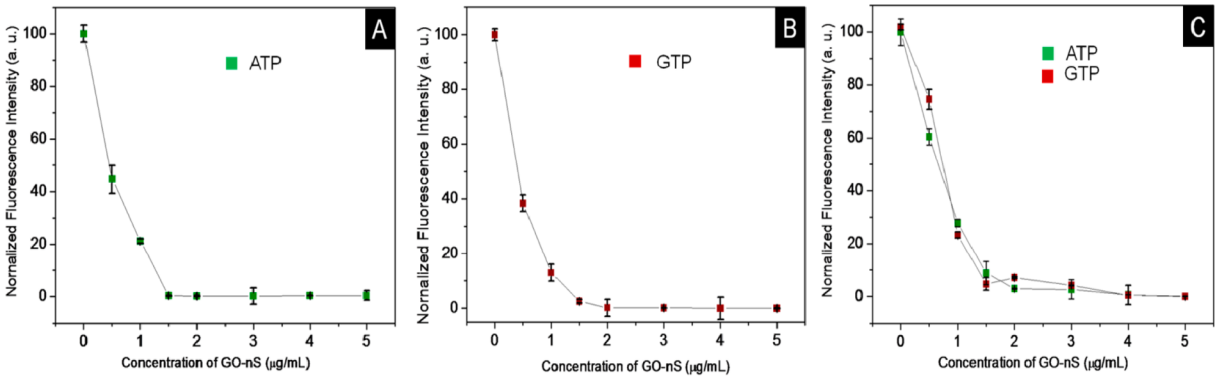

Figure 1. Normalized fluorescence intensity of 100 nM ATP aptamer−FAM (A), 100 nM GTP aptamer−Cy5 (B), and the mixture of 100 nM ATP aptamer−FAM and 100 nM GTP aptamer−Cy5 (C) vs the concentration of GO-nS from 0.5 to 5 μg/mL in reaction buffer. Error bars were obtained from three parallel experiments. Excitation wavelength for FAM, 470 nm; that for Cy5, 650 nm.

and the honeycomb lattice of GO.[30,35−37] As shown in Scheme 1, binding of aptamers to GO-nS guarantees the close proximity of dyes to the graphene surface. The following efficient long-range energy transfer from dye to GO-nS results in rapid and complete quenching of fluorophores. In direct contrast, the conformation of aptamers could be changed into a stable, internal loop structures after interaction with their targets. The weak binding ability of the loop-structured assembly of aptamer/target to GO-nS makes fluorophores far away from the quencher surface, leading to fluorescence recovery of FAM or Cy5. Referring to previous studies about drug delivery and tumor diagnostics using graphene derivates, we proposed that GO-nS could be suitable for visualization of multiple nucleotides based on the fluorescent off/on switch mechanism.[30,34,37] Hence, cell imaging tests were carried out on MCF-7 cells (human breast cancer cell) incubated with aptamer/GO-nS complex consisting of ATP aptamer−FAM, GTP aptamer−Cy5, and GO-nS. The fluorescent signal was captured by a confocal microscope. As a result, the pictures would show bright fluorescent signals corresponding to FAM and Cy5 tagged on DNA/RNA aptamers releasing from the complex after interaction with cellular adenine derivates (including ATP, AMP, and adenine) and guanosine derivates, since both of ATP- and GTP-selective aptamers were in lack of distinguishing adenine and guanosine derivates.

Characterization of GO-nS. GO-nS were demonstrated with smaller size and narrow size distribution relative to GO (Supporting Information Figure S1). To illustrate other features of GO-nS, characterizations of XRD (Supporting Information Figure S2), Raman (Supporting Information Figure S3), and FT-IR spectra (Supporting Information Figure S4) were carried out and detailed in the Supporting Information. TEM images of GO (Supporting Information Figure S5) and GO-nS and aptamer/GO-nS (Supporting Information Figure S6) were illustrated to show their morphology. Detail discussion about GO-nS characterizations are illustrated in the Supporting Information.[51−55]

In Vitro Detection of Multiple Nucleotides. Fluorescence quenching ability of GO-nS was evaluated prior to in vitro detection of ATP and GTP (Figure 1). Single-aptamer/GO-nS complex was formed by mixing 100 nM ATP aptamer−FAM or 100 nM GTP aptamer−Cy5 with 0.5−5 μg/mL GO-nS for 5 min in reaction buffer. The quenching ability of GO-nS to ATP aptamer−FAM (Figure 1A) and GTP aptamer−Cy5 (Figure 1B) was evaluated, respectively. Fluorescence intensity from FAM or Cy5 decreased sharply as increasing concentration of GO-nS due to FRET between fluorophore and GO-nS. Meanwhile, multiaptamer/GO-nS complex including ATP aptamer−FAM and GTP aptamer−Cy5 simultaneously was tested to determine the optimized GO-nS concentration for dual detection of ATP and GTP. As shown in Figure 1C, fluorescence intensity derived from ATP aptamer−FAM and GTP aptamer−Cy5 is mostly being quenched when the concentration of GO-nS reaches 3 μg/mL. However, it is not stable until the concentration of GO-nS is up to 5 μg/mL. Consequently, 5 μg/mL GO-nS was considered optimal for dual probing of ATP and GTP simultaneously, while 3 μg/mL GO-nS was taken as the optimized amount for individual ATP or GTP aptamer.

ATP detection has been performed in our previous study.[30] Herein we are mainly focusing on the dissociation of GTP aptamer−Cy5 from aptamer/GO-nS complex and the resulted fluorescence recovery (Figure 2). As shown in Figure 2A, after 5 min of incubation of GTP aptamer−Cy5 with GO-nS, a nearly 100% fluorescence quenching with very fast kinetics was observed for GTP aptamer−Cy5/GO-nS complexes. On being incubated with 10 μM to 2 mM of GTP for 60 min, GTP aptamer−Cy5 fluorescence was recovered linearly over the range of GTP concentrations (inset of Figure 2A), suggesting that GTP aptamer−Cy5 was specifically liberated from the GO-nS surface. Tracing the cause, the weak binding ability of the loop-structured assembly of aptamer/target to GO-nS makes fluorophores far away from the quencher surface and leads to fluorescence recovery of Cy5. Supporting Information Figure S7 illustrates specific dissociation of GTP aptamer only in the presence of GTP, but not ATP, CTP, or TTP. The large planar surface of GO-nS raise the possibility for adsorption of multiple aptamers whose dissociation could then be specifically monitored using the appropriate Ex/Em wavelengths for FAM and Cy5 dyes (FAM Ex_{495}/Em_{520}; Cy5 Ex_{650}/Em_{670}). As shown in Figure 2B, multiaptamer/GO-nS complex was formed by mixing of 100 nM ATP aptamer−FAM and 100 nM GTP aptamer−Cy5 with 5 μg/mL GO-nS for 5 min in reaction buffer. ATP aptamer−FAM/GTP aptamer−Cy5/GO-nS complex was then incubated with 0.5 and 2 mM ATP, GTP, CTP, or TTP, respectively. Selective release of ATP aptamer or GTP aptamer due to the high specific interaction between aptamer and the target was observed by recording the fluorescence change. However, for CTP and TTP, no obvious change was

dx.doi.org/10.1021/ac400858g | Anal. Chem. 2013, 85, 6775−6782

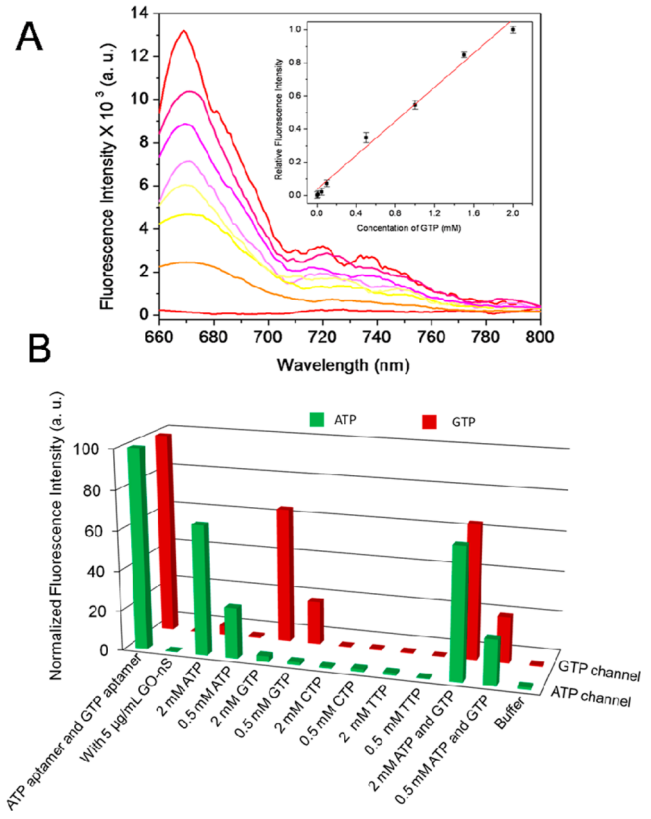

Figure 2. (A) Fluorescence emission spectra of 100 nM GTP aptamer−Cy5 quenched with 3 μg/mL GO-nS (red bottom line) and fluorescence recovery by addition of GTP with concentration ranging from 0.01 to 2 mM (from bottom to top) in reaction buffer for 1 h at 25 °C. Inset: linear relationship between $(F - F_0)/F_0$ (relative fluorescence intensity, where F_0 and F are the fluorescence intensity without and with the presence of GTP) and GTP concentration; error bars were obtained from three parallel experiments. (B) Selective responding to ATP and GTP based on the aptamer/GO-nS sensing platform by recording the respective fluorescence channel (green color presents the FAM channel and red color presents the Cy5 channel). Normalized fluorescence intensity of the mixture of 100 nM ATP aptamer−FAM and 100 nM GTP aptamer−Cy5 in reaction buffer is shown in the column labeled "ATP aptamer and GTP aptamer". After injection of GO-nS, fluorescence was quenched, shown as the column labeled "with 5 μg/mL GO-nS". By incubation of ATP aptamer−FAM/GTP aptamer−Cy5/GO-nS with 0.5 and/or 2 mM ATP, GTP, CTP, or TTP for 1 h at 25 °C, respectively (shown in the corresponding columns), fluorescence recovery was obtained. Excitation wavelength for FAM, 470 nm; that for Cy5, 650 nm.

obtained. This observation successfully facilitates the following ATP/GTP detections inside living cells.

Cleavage Protection and Cell Viability Assay of GO-nS. As we know, most biological probes, such as mRNA and molecular beacons, are easily degraded by cellular enzymes or digested by cellular nucleases, which seriously limits their further applications in living cell studies. Therefore, delivery of aptamer probes into cells while protecting the fluorescent aptamers from enzymatic cleavage is significant to facilitate biological application of aptamers. To date, only a few nanomaterials (such as carbon nanotubes, silica nanoparticles, and gold nanoparticles) have demonstrated with protection capabilities during molecular transport.[43,44,46] Agarose gel electrophoresis was used to demonstrate GO-nS-dependent protection of aptamer from enzymatic cleavage. In order to separate aptamer and GO-nS, electrophoresis was carried out right after heating of the samples at 95 °C for 5 min (Figure 3A). DNase I, which can nonspecifically cleave single- and double-stranded DNA, was employed to simulate enzymatic cleavage functions in living cells. Incubation of ATP aptamer−FAM with DNase I (0.2 units/μL) for 15 or 40 min resulted in cleavage and loss of detection, relative to ATP aptamer−FAM control without any DNase I shown as lane 2 in Figure 3A. In contrast, the ATP aptamer−FAM/GO-nS complex is hard to be cleaved by DNase I after 15 or 40 min of incubation, suggesting that the GO-nS provides strong protecting ability to aptamers against enzymatic cleavage.

To realize the in situ target monitoring in living cells, aptamer/GO-nS complexes are expected to be with good biocompatibility and low toxicity. Consequently, we investigated whether GO-nS reduced cell viability in MCF-7 cells as an initial test case (Figure 3B). MCF-7 cells were incubated with 1−9 μg/mL of GO-nS for 24−72 h, and cell was determined under trypan blue assay, which measures plasma membrane integrity as an index of cell viability. GO-nS showed negligible effects on cell viability at concentrations of ≤7 μg/mL (Figure 3B). Certain toxicity could be observed at the highest concentration (9 μg/mL) by 72 h. The results demonstrated that GO-nS exhibited negligible effects on the growth in MCF-7 cells with concentration lower than 7 μg/mL, while the postculture time was less than 72 h. Cells treated with a large amount of GO-nS for longer culture time resulted in low cell proliferations because of mild cytotoxicity.

In Situ Live Cell Imaging of Multiple Nucleotides. We have demonstrated that multiple aptamers could be adsorbed onto GO-nS while retaining good specificity for their respective triphosphates to dissociate from the aptamer/GO-nS complex. To further test whether this platform could be used for intracellular simultaneous imaging studies, MCF-7 cells were employed to be incubated with multiaptamer/GO-nS consisting of ATP aptamer−FAM, GTP aptamer−Cy5, and random DNA−Alex546N for 6 h. Random DNA−Alex546N was designed as a reference probe to evaluate the specificity of this platform in living cells (Figure 4). MCF-7 cells incubated with ATP aptamer−FAM/GTP aptamer−Cy5/random DNA−Alex546N without assistance of GO-nS were taken as control to prove the transport ability of GO-nS. As shown in Figure 4, fluorescence signal derived from ATP aptamer−FAM and GTP aptamer−Cy5 was clearly observed (Figure 4, parts a and b), while little/no fluorescent signal from the random DNA aptamer could be observed (Figure 4c). Meanwhile, fluorescence could not be observed without GO-nS (Figure 4f−j). In addition, merged images show both colocalization and discrete subcellular localization profiles associated with the ATP and GTP aptamers. Furthermore, MCF-7 cells were incubated with the multiaptamer/GO-nS complex (ATP aptamer−FAM/GTP aptamer−Cy5/random DNA−Alex546N/GO-nS) at concentrations ranging from 50 to 200 nM, and images were captured by a confocal microscope at 6 h postincubations (Figure 5). Fluorescence intensities corresponding to cellular ATP (green color, Figure 5, parts a, e, i, and m) and GTP (red color, Figure 5, parts b, f, j, and n) increased with increasing complex concentration. In contrast, fluorescent signal corresponding to random DNA−Alex546N remained below detection as shown in Figure 5, parts c, g, k, and o. These results demonstrated that this sensing platform could deliver multiple aptamer probes into living cells and successfully realize the in situ visualization of ATP and GTP simultaneously.

dx.doi.org/10.1021/ac400858g | Anal. Chem. 2013, 85, 6775−6782

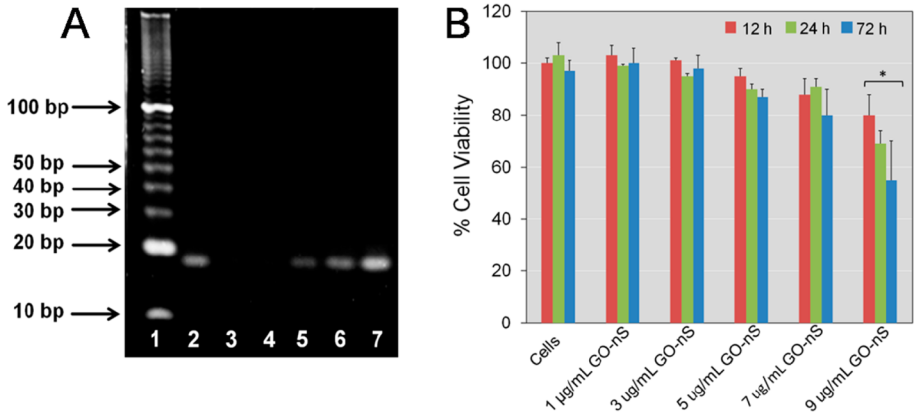

Figure 3. (A) Agarose gel electrophoresis image for enzymatic cleavage protection assay: lane 1, DNA size ladder for 100 bp; lane 2, aptamer−FAM; lane 3, aptamer−FAM reacted with DNase I for 15 min; lane 4, aptamer−FAM reacted with DNase I for 40 min; lane 5, aptamer−FAM/GO-nS; lane 6, aptamer−FAM/GO-nS incubated with DNase I for 15 min; lane 7, aptamer−FAM/GO-nS incubated with DNase I for 40 min. Aptamer concentration is 100 nM, GO-nS is 3 μg/mL, and DNase I is 0.2 units/μL. Excitation wavelength for SYBR green I, 494 nm. (B) Cell viability determined using a trypan blue assay after treatment of MCF-7 cells with 1−9 μg/mL GO-nS for 12 (red), 24 (green), or 72 h (blue). Values represent the mean ± SE, n = 3. *Significantly different from control, $p < 0.05$.

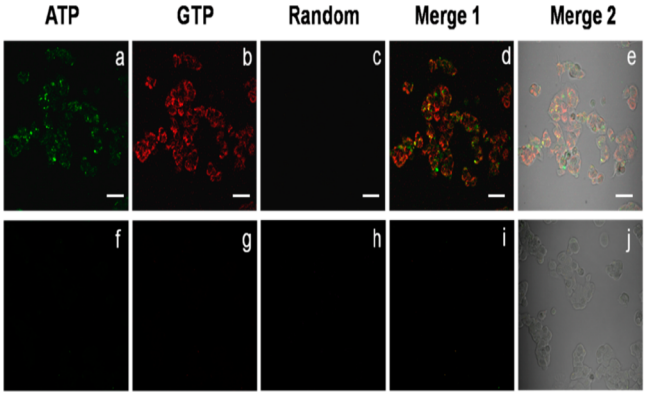

Figure 4. Confocal images of in situ visualization for ATP and GTP. Images represent MCF-7 cells incubated in completed EME medium for 6 h with 100 nM ATP aptamer−FAM/GO-nS (a), 100 nM GTP aptamer−Cy5/GO-nS (b), 100 nM random DNA−Alex546N/GO-nS (c), and the merged fluorescent panels for confocal images (d). Merged confocal images with bright-field image (e). Corresponding images for MCF-7 cells incubated with ATP aptamer−FAM (f), GTP aptamer−Cy5 (g), random DNA−Alex546N (h) alone without assistance of GO-nS, the merged fluorescent panels for confocal images (i), and merged confocal images with bright field image (j) are illustrated. Images were captured by confocal microscope after extensive washing of cells with PBS. Scale bar: 50 μm.

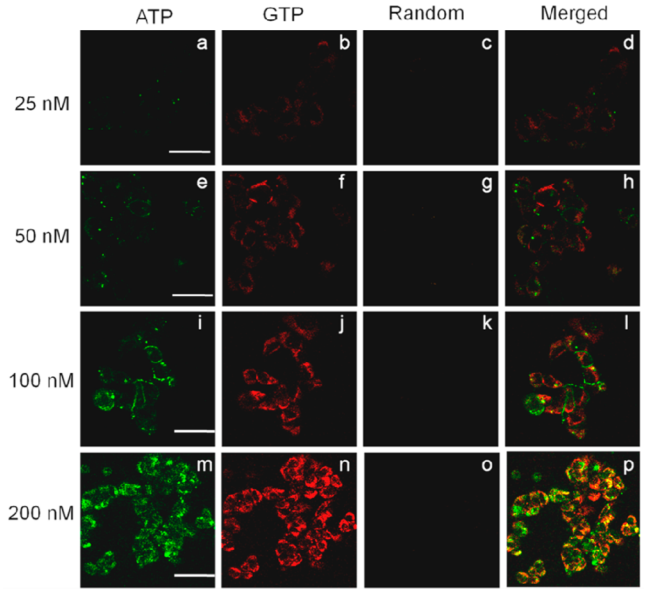

Figure 5. In situ cell imaging of MCF-7 cells with 25 (a−c), 50 (e−g), 100 (i−k), and 200 nM (m−o) ATP aptamer−FAM/GTP aptamer−Cy5/random DNA−Alex546N/GO-nS for 6 h in completed EME medium. Images of cells were captured using the respective Ex/Em wavelengths for each fluorophore and equal exposure times followed by completely rinsing with PBS. Merged images are illustrated in panels d, h, i, and p. Scale bar: 10 μm.

CONCLUSIONS

In summary, an advanced in situ sensing platform for multiple nucleotides detection has been fabricated with DNA/RNA aptamers and GO-nS. GO-nS exhibited strong loading ability to multiple DNA/RNA aptamer probes while their biological functions remained as expected. Meanwhile, GO-nS displayed good biocompatibility to living cells, efficient intracellular transport capacity, and high protecting ability for DNA/RNA probes from enzymatic cleavage. Moreover, the GTP−RNA aptamer utilized in this work would be the foremost demonstration of this RNA aptamer in practical investigation. The positive results achieved here might become an initial guide for the potential applications of this GTP RNA aptamer in biochemical studies. In conclusion, this platform showed great advantages and holds great potential to be applied in many other cellular studies such as multiple imaging of DNA, protein, and RNA, etc. The apparent biocompatibility, efficient intracellular transport capacity, and ability of GO-nS to protect DNA/RNA against cleavage might find important applications in drug delivery and gene therapy associated with predicting biomarkers such as single-nucleotide polymorphisms and microRNAs.

ASSOCIATED CONTENT

Supporting Information

Additional information about synthesis of chemically prepared graphene oxide (GO) and GO-nS, characterizations of GO and

dx.doi.org/10.1021/ac400858g | Anal. Chem. 2013, 85, 6775−6782

GO-nS, and in vivo selective responding of GTP as noted in text. This material is available free of charge via the Internet at http://pubs.acs.org.

AUTHOR INFORMATION

Corresponding Author

*E-mail: jhli@mail.tsinghua.edu.cn (J.L.); Yuehe.Lin@pnnl.gov (Y.L.).

Author Contributions

⊥Dr. Ying Wang and Dr. Zhaohui Li contributed equally to this work.

Notes

The authors declare no competing financial interest.

ACKNOWLEDGMENTS

This work was financially supported by the National Basic Research Program of China (no. 2011CB935704), the National Natural Science Foundation of China (nos. 21235004 and 21128005), and Tsinghua University Initiative Scientific Research Program. This work was supported by a laboratory-directed research and development program at Pacific Northwest National Laboratory (PNNL). Part of the research described in this paper was performed using EMSL. PNNL is operated for DOE by Battelle under contract DE-AC05-76RL01830. The authors are very grateful to Dr. Alan Scott Lea (PNNL), Professor Li Yu (Tsinghua University), Professor Dongsheng Liu (Tsinghua University), and Mr. Yunpeng Huang (Tsinghua University) for professional advice.

REFERENCES

(1) Cassel, D.; Selinger, Z. *Proc. Natl. Acad. Sci. U.S.A.* **1977**, *74*, 3307−3311.
(2) Saraste, M.; Sibbald, P. R.; Wittinghofer, A. *Trends Biochem. Sci.* **1990**, *15*, 430−434.
(3) Ashcroft, S. J. H.; Ashcroft, F. M. *Cell. Signalling* **1990**, *2*, 197−214.
(4) Palleros, D. R.; Reid, K. L.; Shi, L.; Welch, W. J.; Fink, A. L. *Nature* **1993**, *365*, 664−666.
(5) Desai, A.; Verma, S.; Mitchison, T. J.; Walczak, C. E. *Cell* **1999**, *96*, 69−78.
(6) Davies, R. E. *Nature* **1963**, *199*, 1068−1074.
(7) Khakh, B. S.; North, R. A. *Nature* **2006**, *442*, 527−532.
(8) Brake, A. J.; Wagenbach, M. J.; Julius, D. *Nature* **1994**, *371*, 519−523.
(9) Finger, T. E.; Danilova, V.; Barrows, J.; Bartel, D. L.; Vigers, A. J.; Stone, L.; Hellekant, G.; Kinnamon, S. C. *Science* **2005**, *310*, 1495−1499.
(10) Blau, N.; Niederwieser, A. *J. Clin. Chem. Clin. Biochem.* **1985**, *23*, 169−176.
(11) Connolly, T.; Rapiejko, P. J.; Gilmore, R. *Science* **1991**, *252*, 1171−1173.
(12) Scheerer, P.; Park, J. H.; Hildebrand, P. W.; Kim, Y. J.; Krauss, N.; Choe, H. W.; Hofmann, K. P.; Ernst, O. P. *Nature* **2008**, *455*, 497−502.
(13) Prenzel, N.; Zwick, E.; Daub, H.; Leserer, M.; Abraham, R.; Wallasch, C.; Ullrich, A. *Nature* **1999**, *402*, 884−888.
(14) Hogg, T.; Mechold, U.; Malke, H.; Cashel, M.; Hilgenfeld, R. *Cell* **2004**, *117*, 57−68.
(15) Nadler, M. J. S.; Hermosura, M. C.; Inabe, K.; Perraud, A. L.; Zhu, Q. Q.; Stokes, A. J.; Kurosaki, T.; Kinet, J. P.; Penner, R.; Scharenberg, A. M.; Fleig, A. *Nature* **2001**, *411*, 590−595.
(16) Ikeuchi, Y.; Kitahara, K.; Suzuki, T. *EMBO J.* **2008**, *27*, 2194−2203.
(17) Pisareva, V. P.; Pisarev, A. V.; Komar, A. A.; Hellen, C. U. T.; Pestova, T. V. *Cell* **2008**, *135*, 1237−1250.
(18) Li, N.; Ho, C.-M. *J. Am. Chem. Soc.* **2008**, *130*, 2380−2381.
(19) Wang, S. L.; Chang, Y. T. *J. Am. Chem. Soc.* **2006**, *128*, 10380−10381.
(20) McCleskey, S. C.; Griffin, M. J.; Schneider, S. E.; McDevitt, J. T.; Anslyn, E. V. *J. Am. Chem. Soc.* **2003**, *125*, 1114−1115.
(21) Kwon, J. Y.; Singh, N. J.; Kim, H. N.; Kim, S. K.; Kim, K. S.; Yoon, J. Y. *J. Am. Chem. Soc.* **2004**, *126*, 8892−8893.
(22) Ojida, A.; Nonaka, H.; Miyahara, Y.; Tamaru, S. I.; Sada, K.; Hamachi, I. *Angew. Chem., Int. Ed.* **2006**, *45*, 5518−5521.
(23) Li, C.; Numata, M.; Takeuchi, M.; Shinkai, S. *Angew. Chem., Int. Ed.* **2005**, *44*, 6371−6374.
(24) Xu, Z.; Singh, N. J.; Lim, J.; Pan, J.; Kim, H. N.; Park, S.; Kim, K. S.; Yoon, J. *J. Am. Chem. Soc.* **2009**, *131*, 15528−15533.
(25) Chen, D.; Li, J. H. *Chem. Rev.* **2012**, *112*, 6027−6053.
(26) Wang, J.; Jiang, Y. X.; Zhou, C. S.; Fang, X. H. *Anal. Chem.* **2005**, *77*, 3542−3546.
(27) Neelakandan, P. P.; Hariharan, M.; Ramaiah, D. *J. Am. Chem. Soc.* **2006**, *128*, 11334−11335.
(28) Geim, A. K. *Science* **2009**, *324*, 1530−1534.
(29) Zeng, Q.; Cheng, J.; Tang, L.; Liu, X.; Liu, Y.; Li, J. H.; Jiang, J. H. *Adv. Funct. Mater.* **2010**, *20*, 3366−3372.
(30) Wang, Y.; Li, Z. H.; Hu, D. H.; Lin, C. T.; Li, J. H.; Lin, Y. H. *J. Am. Chem. Soc.* **2010**, *132*, 9274−9276.
(31) Wang, Y.; Lu, J.; Tang, L. H.; Chang, H. X.; Li, J. H. *Anal. Chem.* **2009**, *81*, 9710−9715.
(32) Wang, Y.; Li, Y. M.; Tang, L. H.; Lu, J.; Li, J. H. *Electrochem. Commun.* **2009**, *11*, 889−892.
(33) Feng, L.; Wu, L.; Wang, J.; Ren, J.; Miyoshi, D.; Sugimoto, N.; Qu, X. *Adv. Mater.* **2012**, *3*, 125−131.
(34) Liu, Z.; Robinson, J. T.; Sun, X. M.; Dai, H. J. *J. Am. Chem. Soc.* **2008**, *130*, 10876−10877.
(35) Wu, M.; Kempaiah, R.; Huang, P. J.; Maheshwari, V.; Liu, J. W. *Langmuir* **2011**, *27*, 2731−2738.
(36) Huang, P. J.; Liu, J. W. *Anal. Chem.* **2012**, *84*, 4192−4198.
(37) Lu, C. H.; Zhu, C. L.; Li, J.; Liu, J. J.; Chen, X.; Yang, H. H. *Chem. Commun.* **2010**, *46*, 3116−3118.
(38) He, S. J.; Song, B.; Li, D.; Zhu, C. F.; Qi, W. P.; Wen, Y. Q.; Wang, L. H.; Song, S. P.; Fang, H. P.; Fan, C. H. *Adv. Funct. Mater.* **2010**, *20*, 453−459.
(39) Nie, H. H.; Liu, S. J.; Yu, R. Q.; Jiang, J. H. *Angew. Chem., Int. Ed.* **2009**, *48*, 9862−9866.
(40) Wu, Z.; Zhen, Z.; Jiang, J. H.; Shen, G. L.; Yu, R. Q. *J. Am. Chem. Soc.* **2009**, *131*, 12325−12332.
(41) Huang, Y.; Zhang, Y. L.; Xu, X.; Jiang, J. H.; Shen, G. L.; Yu, R. Q. *J. Am. Chem. Soc.* **2009**, *131*, 2478−2480.
(42) Zhang, Y. L.; Wang, Y.; Wang, H. B.; Jiang, J. H.; Shen, G. L.; Yu, R. Q.; Li, J. H. *Anal. Chem.* **2009**, *81*, 1982−1987.
(43) Fang, X. H.; Tan, W. H. *Acc. Chem. Res.* **2010**, *43*, 48−57.
(44) Song, S.; Wang, L.; Li, J.; Zhao, J.; Fan, C. *Trends Anal. Chem.* **2008**, *27*, 108−117.
(45) Huizenga, D. E.; Szostak, J. W. *Biochemistry* **1995**, *34*, 656−665.
(46) Liu, J. W.; Cao, Z. H.; Lu, Y. *Chem. Rev.* **2009**, *109*, 1948−1998.
(47) Carothers, J. M.; Oestreich, S. C.; Szostak, J. W. *J. Am. Chem. Soc.* **2006**, *128*, 7929−7937.
(48) Davis, J. H.; Szostak, J. W. *Proc. Natl. Acad. Sci. U.S.A.* **2002**, *99*, 11616−11621.
(49) Carothers, J. M.; Oestreich, S. C.; Davis, J. H.; Szostak, J. W. *J. Am. Chem. Soc.* **2004**, *126*, 5130−5137.
(50) Carothers, J. M.; Davis, J. H.; Chou, J. J.; Szostak, J. W. *RNA* **2006**, *12*, 567−579.
(51) Chen, D.; Feng, H. B.; Li, J. H. *Chem. Soc. Rev.* **2012**, *112*, 6027−6053.
(52) Lv, X. J.; Fu, W. F.; Chang, H. X.; Zhang, H.; Cheng, J. S.; Zhang, G. J.; Song, Y.; Hu, C. Y.; Li, J. H. *J. Mater. Chem.* **2012**, *22*, 1539−1546.
(53) Tang, L. H.; Wang, Y.; Liu, Y.; Li, J. H. *ACS Nano* **2011**, *5*, 3817−3822.
(54) Dreyer, D. R.; Park, S.; Bielawski, C. W.; Ruoff, R. S. *Chem. Soc. Rev.* **2010**, *39*, 228−240.

(55) Wang, Y.; Zhang, S.; Du, D.; Shao, Y. Y.; Li, Z. H.; Wang, J.; Engelhard, M. H.; Li, J. H.; Lin, Y. H. *J. Mater. Chem.* **2011**, *21*, 5319−5325.